





Research on Planning Method of Rural High-Density Building Group Based on Tree Structure Simulation Algorithm

Jingwen Wang^{1*} and Zhaozhao Huang²

¹College of Engineering, Zhengzhou Technology and Business University, Zhengzhou, Henan 450001, China

¹simple6475@163.com, ²Zhaozhao_Huang2022@163.com

Corresponding author: Jingwen Wang, simple6475@163.com

Abstract: In order to improve the planning effect of rural high-density building groups, this paper combines the tree structure simulation algorithm to analyze the planning and analysis of rural high-density building groups, proposes a new potential function clustering formula, and proposes a hybrid matrix estimation algorithm based on single-source point detection. Moreover, this paper uses STFT to realize the sparse representation of the observation signal, and removes the time-frequency points that are greatly affected by noise. In addition, this paper further filters the time-frequency points according to the single-source point detection criterion, and uses the obvious clustering features of the time-frequency ratio of the frequency-hopping signal at the single-source point to obtain the estimation of the mixing matrix of each hop signal, and finally obtain the DOA estimated value. The simulation results show that the algorithm has better estimation performance than the comparison algorithms. Finally, through the simulation experiments, it is verified that the planning method of rural high-density building groups based on the tree structure simulation algorithm can effectively improve the planning effect.

Keywords: tree structure; simulation algorithm; countryside; high density; building complex; planning

DOI: <https://doi.org/10.14733/cadaps.2023.S15.163-181>

1 INTRODUCTION

It is urgent to solve the problem of resettlement of landless farmers. However, the current research on landless farmers is basically concentrated in two fields—management and sociology. There is a lack of practical strategies, principles and methods for the design of housing environment that are closely related to landless farmers. Settlement is a result of the mutual adaptation of human beings and the natural environment. After thousands of years of coordination, various settlement forms,

architectural styles, architectural layouts, etc. have been produced. We should study the essential laws behind these things, then learn it and make it serve our modern life.

The design and design of the existing resettlement areas are completely copied from foreign design methods. These methods introduced from abroad are first used in the city. Due to the development of the economy, the dual opposition between urban and rural areas has persisted for a long time. The economic culture, production and lifestyle, customs and habits of urban and rural areas are completely different. It is obviously not feasible to completely transplant the design method of urban communities to rural resettlement communities[7]. The location of the centralized resettlement area is mainly in the suburbs or suburbs of the city, regardless of the surrounding environment, topography, environmental resources, etc. The layout of the resettlement area is rigid and single, basically a determinant layout, and the space is extremely homogenized. Due to the hurried construction period, the construction speed is very fast, instead of carefully exploring the individual needs of the people who will live in it, it is directly mass-produced[8]. The exterior design of the resettlement area only seeks to look good without considering the collective consciousness of the original residents, which is a kind of contempt for the original production and living space [12]. The exclusive small courtyard-style neighborhood communication space that farmers used to have disappeared, leaving only a row of barracks-style houses, and the public leisure space is a mere formality and has no practical effect. The landscape is only covered with turf to dress up, and if there is other needs in the later stage, it will be changed directly. The common practice is to transform it into a parking lot [15]. In general, the design of the existing resettlement community does not dig deeply into the individualized life of the common people, and lacks consideration of the living habits and customs of the farmers, so that the design is not based on the real needs of the common people, which makes the residents in the resettlement area not. There is no sense of belonging to the community, the relationship between neighbors is lost, and people are indifferent [4].

As one of the most important types of artificial objects in the basic geographic database, buildings change most frequently, so they need to be updated in time. At the same time, buildings are also one of the most widely distributed and important objects in urban and rural remote sensing images. Since the way of manually interpreting and extracting buildings is time-consuming and labor-intensive, how to use computers to automatically extract buildings has become a research hotspot. There are two main categories of methods for automatically extracting buildings: bottom-up data-driven methods and top-down model-driven methods [10]. The data-driven method refers to taking the ground features as a combination of many underlying features, and extracting the target features through artificially designed feature rules. At present, it mainly includes based on geometric boundary, based on region segmentation, based on auxiliary information and so on. Among them, the method based on geometric boundary is: extracting buildings on suburban images by combining rectangular boxes and building shadows [14]. The significance of high-resolution remote sensing image processing and analysis based on feature primitives is analyzed theoretically and practically, and a technical framework for multi-scale information extraction of high-resolution remote sensing images based on feature primitives is proposed [16]. Using multiple aerial remote sensing images to extract flat roof and gable roof, and combine and filter the extraction results by wall and shadow information [11]. The geometric features and grayscale features of buildings are extracted, the contour line segments are selected according to their spatial distribution characteristics and Hough transform characteristics, and the extraction results are used as the basis for judging the building target, and finally the building is accurately extracted [13]. For example, a method based on region segmentation: a combination of Canny operator-based multi-scale segmentation and edge segmentation is proposed to segment and extract buildings [2]. Auxiliary information based methods such as: extracting target buildings from DSM data by improving the marker control method for watershed segmentation [8]. Using the method of oblique photogrammetry, combined with multi-view images to extract the texture information of the building wall, a good 3D reconstruction result of the building has been achieved [18].

There are different types of planning systems, including main functional area planning, urban and rural planning, land use planning, ecological environmental protection and other planning types. The main functional area planning is mainly divided into four types according to the land use value, namely priority development, key development, restricted development, and prohibited development. According to the level, it is divided into national main function planning and provincial main function planning. Urban and rural planning is divided into overall planning, special planning, and regional planning according to functional types. The overall planning is based on the distribution of population resources in cities, counties, and townships and the overall social and economic planning. Regional planning is based on the overall planning. Planning, special planning is a specific planning for the specific function types of the overall planning, and it is a detailed division of the overall planning [3]. Land use planning, like urban and rural planning, is divided into three categories according to functional types: general land planning, detailed land planning, and special land planning. The three are complementary and closely related to each other. Ecological environmental protection planning is divided into ecological environment special planning and ecological environmental protection planning. The former is mainly for a detailed plan for different types of ecological resources, and the latter is mainly for the protection of ecological resources. In the past, the four types of planning were separate from each other, and the repetition was very strong. In the planning process, it was easy to be intertwined with each other. At the same time, there were many approval procedures, and large-scale projects required layer-by-layer approval. Land and spatial planning is a process of combining and simplifying these four types of planning [1]. It is mainly implemented in three steps, namely, unifying the base map, improving the basic information platform of land and space, and controlling the use of land and space. In the past, different plans used their own drawings, while land and space planning requires a unified base map for various types of plans, superimposing the approved planning on a system platform, and then uploading the results of the planning stage to the land and space basic information platform. , the last step is to control the use of the perfect drawing information [5].

Architectural features are the overall spatial characteristics of a settlement formed under the combined action of geographical and historical factors, including street and lane patterns, site images, courtyard shapes, architectural forms, public landscapes, and even land use patterns and farming forms. The development process of Chinese architecture is divided into structures: cave dwellings, nest dwellings, logging for sheds, Qin brick and Han tiles, wooden structures, brick-timber structures, and reinforced concrete structures [17]. According to the architectural style, it is divided into traditional village style, tourist style, general style, mixed style and single style. Most of the traditional village buildings were built by local craftsmen in the late Qing Dynasty. The tourist village is built by the mountains and rivers, and the surrounding environment is very good. The villagers mainly rely on tourists' consumption as their source of income, and the geographical location is generally relatively remote. The general style is mainly the houses built spontaneously by villagers after the reform and opening up, and the style has the attributes of personal preference [6].

This paper combines the tree structure simulation algorithm to analyze the planning and analysis of rural high-density building groups, and improves the planning effect of rural high-density building groups through intelligent methods.

2 FEATURE EXTRACTION OF RURAL HIGH-DENSITY BUILDING GROUPS

2.1 UBSS Mathematical Model for Feature Information of Frequency Hopping Rural High-Density Building Groups

Most of the existing blind source separation problems model the feature information of rural high-density building groups as a linear mixture for research. At present, the main hybrid methods include linear instantaneous, linear delay and linear convolution. Among them, the delay mixing can fully

describe the transmission delay features of the feature information of frequency hopping rural high-density buildings reaching different receivers. Therefore, a linear time-delay mixed model is used for the study. If it is assumed that the M-element array antenna receives the feature information of N synchronous and orthogonal frequency hopping source rural high-density building groups in the receiving period Δt , and it is assumed that the DOA of the feature information of different rural high-density building groups is different, the linear delay hybrid model based on UBSS can be expressed as:

$$\mathbf{x}(t) = \mathbf{A}(t)\mathbf{s}(t) + \mathbf{v}(t) \quad (1)$$

Among them, $\mathbf{x}(t) = [x_1(t), x_2(t), \dots, x_M(t)]^T$ is the feature information of the receiving rural high-density building group, $\mathbf{A}(t) = [\mathbf{a}_1, \mathbf{a}_2, \dots, \mathbf{a}_N] \in \mathbb{C}^{M \times N}$ is the mixing matrix, and the (m,n)-th element $a_{mn} = e^{-j\omega_n(t)\tau_{mn}} = e^{-j2\pi f_n(t)\tau_{mn}}$, τ_{mn} in $\mathbf{A}(t)$ is the relative delay of the feature information $s_n(t)$ of the nth rural high-density building group reaching the m-th array element. At the same time, $\mathbf{s}(t) = [s_1(t), s_2(t), \dots, s_N(t)]^T$ is the feature information of the high-density building group in the source village, and $\mathbf{v}(t)$ is the Gaussian white noise. The above equation is written in matrix form:

$$\begin{bmatrix} x_1(t) \\ \vdots \\ x_M(t) \end{bmatrix} = \begin{bmatrix} 1 \cdots 1 \\ \vdots \cdots \vdots \\ e^{-j2\pi f_1(t)(M-1)d \sin(\theta_1)c} \cdots e^{-j2\pi f_N(t)(M-1)d \sin(\theta_N)c} \end{bmatrix} \begin{bmatrix} s_1(t) \\ \vdots \\ s_N(t) \end{bmatrix} \quad (2)$$

It can be seen from the mixed model that the mixed matrix $\mathbf{A}(t)$ is related to the DOA of the feature information of rural high-density building groups. Therefore, the DOA can be solved by using the mixed matrix $\mathbf{A}(t)$ of SCA through the UBSS model to achieve the purpose of network station sorting. In this way, the DOA estimation problem of feature information of rural high-density building groups is transformed into a mixture matrix estimation problem under the UBSS model.

The general UBSS algorithm requires the mixing matrix to be fixed, but $\mathbf{A}(t)$ in formula (2) does not meet this requirement due to the working features of the feature information of the high-density building groups in the frequency-hopping rural areas. In order to make the mixing matrix fixed, we limit the data processed each time to the feature information of a single-hop rural high-density building group, that is, between two adjacent hops. The parameters such as time hopping and hopping period of the feature information of the frequency-hopping rural high-density building group can be estimated by the algorithm, and according to these parameters, the received data can be divided into multiple single-hop rural high-density building group feature information. The mixture model can be rewritten as:

$$\mathbf{x}(t) = \mathbf{A}\mathbf{s}(t) + \mathbf{v}(t) \quad (3)$$

Due to the sparseness of the feature information of high-density building groups in frequency-hopping rural areas in the time-frequency domain, the time-frequency transformation is performed on both sides of the above equation. Here, STFT is used to obtain a hybrid model in the time-frequency domain of UBSS for the feature information of frequency-hopping rural high-density building groups:

$$\mathbf{X}(t, f) = \mathbf{A}\mathbf{S}(t, f) + \mathbf{V}(t, f) \quad (4)$$

Among them, $\mathbf{X}(t, f) = [X_1(t, f), X_2(t, f), \dots, X_M(t, f)]^T$, $\mathbf{S}(t, f) = [S_1(t, f), S_2(t, f), \dots, S_N(t, f)]^T$ and $\mathbf{V}(t, f)$ are the time-frequency representation of the feature information of the receiving rural high-density building group, the feature information of the source rural high-density building group and the noise, respectively.

The definition of a single source point is given below: for any time-frequency point (t, f) that satisfies $\|\mathbf{X}(t, f)\|_2^2 > 0$, if there is $|S_n(t, f)| \gg |S_i(t, f)|, n \neq i$, it is considered that there is only the source rural high-density building group feature information $s_n(t, f)$ on (t, f) . It is called the time-frequency single-source point of $s_n(t, f)$, and is referred to as the single-source point for short. Generally, SCA is used to solve the sorting problem of feature information of high-density building complexes in frequency-hopping rural areas, and it also needs to meet the following assumptions of SCA: (1) $\mathbf{R}^{M \times M}$ is non-singular. Among them, $\mathbf{R}^{M \times M}$ is any sub-matrix in \mathbf{A} ; (2) The existence of time-frequency points (t, f) in $s(t, f)$ conforms to the above definition of single source point.

2.2 Hybrid Matrix Estimation Algorithm Based on Single Source Point Detection

In order to facilitate the analysis, we take the observation of the feature information of three source rural high-density building groups by two antenna array elements as an example, and the observation time-frequency matrix of formula (4) can be expressed as

$$\begin{bmatrix} X_1(t, f) \\ X_2(t, f) \end{bmatrix} = \begin{bmatrix} \mathbf{I} & \mathbf{I} & \mathbf{I} \\ a_{21} & a_{22} & a_{23} \end{bmatrix} \begin{bmatrix} S_1(t, f) \\ S_2(t, f) \\ S_3(t, f) \end{bmatrix} \quad (5)$$

In order to avoid the influence of low-energy points caused by noise on the estimation of the mixing matrix, and to reduce the calculation amount of subsequent processing, the noise energy threshold ε_1 is set after STFT, and the time-frequency points with smaller modulus values are removed according to the following formula:

$$X(t_p, f_q) = \begin{cases} X(t_p, f_q), & |X(t_p, f_q)| > \varepsilon_1 \max(X(t, f)) \\ 0, & \text{else} \end{cases} \quad (6)$$

In the above formula, $p=1,\dots,P$ is the time sampling point, $q=1,\dots,Q$ is the frequency sampling point, and ε_l generally takes $0.1 \sim 0.4$.

If it is assumed that a certain time-frequency point (t_p, f_q) is the single source point of the feature information $s_l(t)$ of the rural high-density building group, the time-frequency ratio of receiving the feature information of the rural high-density building group is:

$$\frac{X_2(t_p, f_q)}{X_1(t_p, f_q)} = \frac{a_{2l} S_l(t_p, f_q)}{S_l(t_p, f_q)} = a_{2l} \quad (7)$$

Then, the mixing matrix A can be represented by the time-frequency ratio of the feature information of the rural high-density building group observed at a single source point:

$$A = \begin{bmatrix} 1 & 1 & 1 \\ \frac{X_2(t_p, f_q)}{X_1(t_p, f_q)} & \frac{X_2(t_{p'}, f_{q'})}{X_1(t_{p'}, f_{q'})} & \frac{X_2(t_{p^*}, f_{q^*})}{X_1(t_{p^*}, f_{q^*})} \end{bmatrix} \quad (8)$$

In the above formula, $(t_{p'}, f_{q'})$ and (t_{p^*}, f_{q^*}) are the single source points of the feature information $s_2(t)$ and $s_3(t)$ of the source rural high-density building group, respectively. It can be seen that the time-frequency ratio of the received data at the single source point can describe the mixing matrix relatively completely, so the determination of the single source point is very important for the estimation of the mixing matrix A.

If it is assumed that a certain time-frequency point (t_p, f_q) is the single source point of the feature information $s_l(t)$ of the rural high-density building group, that is, only $s_l(t)$ plays a role in (t_p, f_q) , the time-frequency ratio of receiving the feature information of the rural high-density building group is:

$$\frac{X_2(t_p, f_q)}{X_1(t_p, f_q)} = a_{2l} = e^{-j2\pi f_l(t)\tau_{2l}} \quad (9)$$

$$\frac{X_1(t_p, f_q)}{X_2(t_p, f_q)} = \frac{1}{a_{2l}} = \frac{1}{e^{-j2\pi f_l(t)\tau_{2l}}} \quad (10)$$

According to formula (9) and formula (10), we can get:

$$\left| \frac{X_2(t_l, f_l)}{X_1(t_l, f_l)} \right| - \left| \frac{X_1(t_l, f_l)}{X_2(t_l, f_l)} \right| = 0 \quad (11)$$

The effect of noise is taken into account, and a threshold ε_2 is introduced to broaden the usage conditions:

$$\left| \frac{X_2(t_l, f_l)}{X_1(t_l, f_l)} \right| - \left| \frac{X_1(t_l, f_l)}{X_2(t_l, f_l)} \right| < \varepsilon_2 \quad (12)$$

Among them, there is $0 < \varepsilon_2 \ll 1$.

Now, we prove that formula (11) is no longer satisfied at multiple source points (MSPs). Multi-source point refers to the time-frequency point that has two or more source village high-density building

group feature information. If $(t_{\bar{p}}, f_{\bar{q}})$ is a multi-source point of $S_1(t)$ and $S_2(t)$, there are:

$$\frac{X_2(t_{\bar{p}}, f_{\bar{q}})}{X_1(t_{\bar{p}}, f_{\bar{q}})} = \frac{a_{21}S_1(t_{\bar{p}}, f_{\bar{q}}) + a_{22}S_2(t_{\bar{p}}, f_{\bar{q}})}{S_1(t_{\bar{p}}, f_{\bar{q}}) + S_2(t_{\bar{p}}, f_{\bar{q}})} \quad (13)$$

$$\frac{X_1(t_{\bar{p}}, f_{\bar{q}})}{X_2(t_{\bar{p}}, f_{\bar{q}})} = \frac{S_1(t_{\bar{p}}, f_{\bar{q}}) + S_2(t_{\bar{p}}, f_{\bar{q}})}{a_{21}S_1(t_{\bar{p}}, f_{\bar{q}}) + a_{22}S_2(t_{\bar{p}}, f_{\bar{q}})} \quad (14)$$

In order to make formula (11) still hold, the following formula needs to be satisfied:

$$\left| \frac{a_{21}S_1(t_{\bar{p}}, f_{\bar{q}}) + a_{22}S_2(t_{\bar{p}}, f_{\bar{q}})}{S_1(t_{\bar{p}}, f_{\bar{q}}) + S_2(t_{\bar{p}}, f_{\bar{q}})} \right| = 1 \quad (15)$$

We set $\Delta = a_{21} - a_{22}$. $S_1(t_{\bar{p}}, f_{\bar{q}})$ is abbreviated as S_1 , $S_2(t_{\bar{p}}, f_{\bar{q}})$ is abbreviated as S_2 , and the left-hand side of the above equation can be written as:

$$\begin{aligned} \left| \frac{a_{21}S_1 + a_{22}S_2}{S_1 + S_2} \right| &= \left| \frac{a_{21}S_1 + (a_{21} - \Delta)S_2}{S_1 + S_2} \right| = \left| \frac{a_{21}(S_1 + S_2) - \Delta S_2}{S_1 + S_2} \right| \\ &= \left| a_{21} - \frac{\Delta S_2}{S_1 + S_2} \right| \end{aligned} \quad (16)$$

At the same time, because of $|a_{21}| = 1$, if formula (16) is to be equal to 1, there are two situations as follows:

Case (1): there is $\frac{\Delta S_2}{S_1 + S_2} = 0$.

Because S_2 is non-zero, in this case, there is $\Delta = 0$, that is $a_{21} = a_{22}$.

Case (2): there is $\frac{\Delta S_2}{S_1 + S_2} = a_{21} - (\sin \theta + i \cos \theta)$. Among them, θ is an arbitrary angle. We further extend the above formula to get the following formula:

$$a_{21}S_2 - a_{22}S_2 = a_{21}S_1 + a_{21}S_2 - (\sin \theta + i \cos \theta)(S_1 + S_2) \quad (17)$$

We adjust the factor position to get:

$$a_{21}S_1 + a_{22}S_2 = (\sin \theta + i \cos \theta)(S_1 + S_2) \quad (18)$$

Therefore, in this case, there is $a_{21} = a_{22} = \sin \theta + i \cos \theta$.

The above two situations are synthesized, it can be seen that the conditions for the establishment of formula (11) at the multi-source point are:

$$a_{21} = a_{22} \quad (19)$$

The above conditions are too strict in practical applications, which can be regarded as impossible events, so the multi-source point does not satisfy formula (11).

It is still assumed that the time-frequency point (t_p, f_q) is the single source point of the feature information $S_1(t)$ of the rural high-density building group, the parameter α is defined as:

$$\alpha = \text{angle} \left(\frac{X_2(t_p, f_q)}{X_1(t_p, f_q)} \right) = \text{angle}(a_{21}) = -2\pi f_1 \tau_{21} \quad (20)$$

The potential function clustering algorithm does not need to predict the number of classes, nor to initialize the cluster centers, and it has high precision and high speed in solving one-dimensional parameter problems. Therefore, this chapter uses a potential function to cluster the values of the time-frequency ratio at a single source point. The general form of potential function clustering is:

$$\psi(\Delta) = \sum \gamma \varphi(\Delta) \quad (21)$$

Among them, γ is the energy weight factor, and Δ is the distance from the data to the cluster center. For a one-dimensional vector, Δ is the absolute value of the difference. $\varphi(\Delta)$ is the basis function, which has the following forms:

$$\varphi(\Delta) = \left(e^{-\frac{\Delta}{\sigma}} \right)^\beta \quad (22)$$

$$\varphi(\Delta) = \frac{1}{1 + (\Delta/\sigma)^\beta} \quad (23)$$

$$\varphi(\Delta) = 1 - \frac{\lambda\Delta}{k}, \lambda\Delta < k \quad (24)$$

It can be concluded that the general principle of the potential function clustering algorithm is: when the parameter to be estimated is close to the actual value, the distance Δ tends to 0, the basis function $\varphi(\Delta)$ tends to 1, and $\psi(\Delta)$ reaches the maximum value. When the parameter to be estimated is far from the actual value Δ and becomes larger, the basis function $\varphi(\Delta)$ becomes smaller, and $\psi(\Delta)$ becomes smaller. Therefore, the parameter to be estimated can be determined according to the peak position of $\psi(\Delta)$.

Based on the above principles, the potential function clustering formula proposed in this chapter is:

$$\psi(\alpha) = \sum_{i \in (t_p, f_q)} a^{|\alpha - \alpha_i|} \quad (25)$$

The parameter a affects the decay speed of the basis function $\varphi(\Delta)$ curve, as well as the peak amplitude and curve smoothness of $\psi(\Delta)$. A smaller a makes the peak position closer to the real situation, while it may lead to spurious peaks. The larger a is, the smoother the curve is without spurious peaks, but the peak position is inaccurate. We can determine the value of a based on the results of multiple experiments. When there is no spurious peak, the smaller a is, the better. We can also determine the value according to the following equation:

$$a = \arg \min \left[\sum_{i \in (t_p, f_q)} \min(|\alpha_i - E_1|, |\alpha_i - E_2|, |\alpha_i - E_3|) \right] \quad (26)$$

In the above formula, E_1, E_2, E_3 is the estimated cluster center, the parameter a can be 0.1, 0.01, 0.001, etc., and N is the number of cluster centers.

According to the peak position of the potential function curve, we can estimate the cluster center E_1, E_2, E_3 . The mixing matrix estimate of the received data at this hop is obtained according to the following formula:

$$A_E = \begin{bmatrix} III \\ e^{jE_1} e^{jE_2} e^{jE_3} \end{bmatrix} \quad (27)$$

However, our ultimate goal is to solve the DOA of the feature information of rural high-density building groups. If it is assumed that the feature information of different source rural high-density building groups has different DOAs, according to formula (2), the direction of arrival of the feature information of the n th source rural high-density building group can be obtained as:

$$\theta_n = \arcsin\left(\frac{-\text{angle}(e^{jE_n})c}{2\pi f_n d}\right) \quad (28)$$

However, there is a problem with using the above formula to solve θ_n . We cannot map the feature information carrier frequency values of rural high-density building groups to the estimated mixing matrix elements one-to-one. To solve this problem, we do the following:

The time-frequency domain data of one of the frequencies are selected separately, and the corresponding approximate value a_{mn}' of the mixing coefficient is calculated according to formula (7). a_{mn}' and e^{jE_n} are compared, and the carrier frequency corresponding to e^{jE_n} is determined according to the degree of approximation.

On the basis of single-source point detection and potential function clustering, the algorithm steps for solving the feature information DoA of high-density building groups in frequency-hopping rural areas by using mixture matrix estimation are as follows:

- (1) We process it separately according to the feature information of each hop of rural high-density building groups;
- (2) $x_m(t)$ is subjected to STFT to obtain a time-frequency matrix $X_m(t, f)$;
- (3) We set the noise energy threshold ε_1 to remove low energy points;
- (4) According to the algorithm, the estimated value of the carrier frequency is obtained, and the corresponding approximate value a_{mn}' of the mixing coefficient is calculated;
- (5) According to formula (12), the time-frequency point is detected by a single source point;
- (6) We perform potential function clustering on the corner $\alpha = \text{angle}\left(\frac{X_2}{X_1}\right)$ of the time-frequency ratio at the single source point, and estimate the mixture matrix A_E according to the clustering result and formula (27);
- (7) The approximate value a_{mn}' of the mixing coefficient and the element e^{jE_n} in the estimated mixing matrix are compared to determine the carrier frequency value corresponding to e^{jE_n} ;
- (8) According to formula (28), the DOA of the feature information of each rural high-density building group is calculated;
- (9) According to the DOA, the splicing of the feature information of each rural high-density building group is completed.

2.3 Simulation Analysis

The receiving end of this simulation experiment is a uniform linear array with the number of antenna elements $M=2$, and the spacing d of each array element is half of the shortest wavelength for receiving feature information of high-density buildings in rural areas. The feature information of the high-density building group in the source village adopts the synchronous orthogonal networking mode and adopts BPSK modulation. The number of feature information of rural high-density building groups is $N=3$, the hopping speed is 1000 hops/second, and the arrival angles of feature information

of rural high-density building groups are 20° , 60° , and 80° . The frequency hopping frequency set is shown in formula (29), and the sampling frequency is $f_s = 20\text{MHz}$. We take the first hop to observe the feature information of rural high-density building groups as an example for analysis.

$$f_c = \begin{bmatrix} 862 \\ 6.53.55 \\ 7.516 \end{bmatrix} \text{MHz} \quad (29)$$

According to formula (2), the mixing matrix is obtained as:

$$A = \begin{bmatrix} 111 \\ 0.4762 - 0.8793i - 0.5970 - 0.8022i - 0.9711 - 0.2388i \end{bmatrix} \quad (30)$$

We use STFT as the sparse representation method, the Hamming window with a length of 1024 points is used as the window function, the step length of the window function is 512 points, and the number of Fourier transform points is 1024 points. We set the noise energy threshold $\varepsilon_1 = 0.2$ and the single-source detection threshold $\varepsilon_2 = 0.1$. Figures 1 and 2 show the real and imaginary

scattergrams of the time-frequency ratio $\frac{X_2(t, f)}{X_1(t, f)}$ after observing the feature information of rural high-density building groups and single-source point detection when the signal-to-noise ratio is 5dB . After comparison, it can be seen that the time-frequency ratio data has obvious clustering features after single-source point detection.

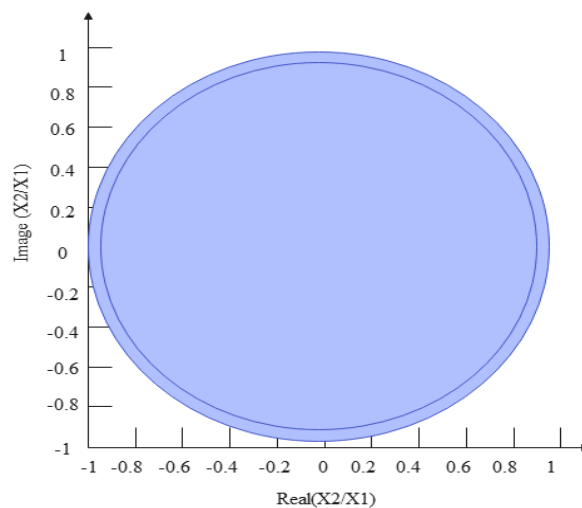


Figure 1: Scatter plot of the real and imaginary parts of the time-frequency ratio of the feature information of the original rural high-density building groups.

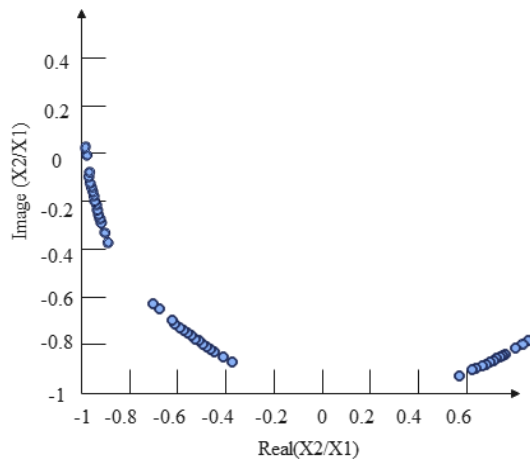


Figure 2: Scatter plot of real and imaginary parts of time-frequency ratio after SSP.

Then, we use formula (25) to perform potential function clustering on the angle $\alpha = \text{angle}\left(X_2(t_p, f_q) / X_1(t_p, f_q)\right)$ of the data time-frequency ratio in Figure 2. Different basis functions are used to obtain different clustering results and performance. Therefore, it is necessary to select the value of the basis function according to the cluster center estimation error corresponding to different basis functions.

$$e_r = \sum_{i \in (t_p, f_q)} \left(\min(|\alpha_i - E_1|, |\alpha_i - E_2|, |\alpha_i - E_3|) \right)^2$$

The cluster center estimation error is defined.

Among them, the parameter a takes the value $10^{-1}, 10^{-2}, 10^{-3}, 10^{-4}, 10^{-5}, 10^{-6}, 10^{-7}, 10^{-8}$, and the error calculated using each basis function is shown in Figure 3.

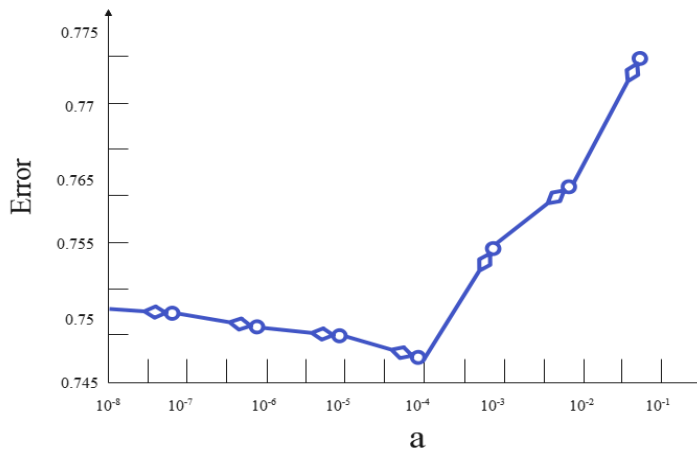


Figure 3: Errors between cluster centers and samples obtained by different basis functions.

It can be seen from the above figure that when there is $a = 10^{-4}$, the optimal cluster center estimation result can be obtained, so $\varphi(\Delta) = (10^{-4})^{\Delta}$ is selected as the basis function of the simulated experimental potential function in this chapter. The final obtained potential function $\psi(\alpha)$ varies with α as shown in Figure 4.

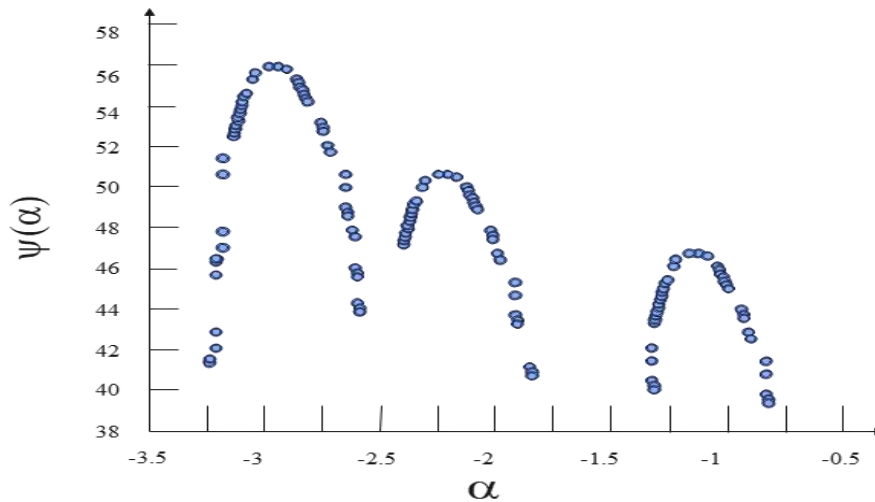


Figure 4 : The curve diagram of the change of $\psi(\alpha)$ with α

Since the number of feature information of high-density building groups in the source village is 3, it can be clearly seen that there are 3 peaks in the above figure. According to the abscissa position of the peak point, the cluster center of α is determined, and then the mixture matrix is estimated according to formula (27).

In order to evaluate the estimation performance of the mixture matrix based on the single-source point detection and potential function clustering algorithm in this chapter, the normalized mean square error of the mixture matrix is defined as

$$NMSE = 10 \log_{10} \frac{\sum_{m,n} |(a_{mn} - \tilde{a}_{mn})|^2}{\sum_{m,n} |(a_{mn})|^2} \quad (31)$$

In the above formula, a_{mn}, \tilde{a}_{mn} is the true value and estimated value of the mixing coefficient, respectively. Figure 5 is a graph showing the variation of NMSE with the signal-to-noise ratio of the algorithm proposed in this paper and the algorithm in the literature under the signal-to-noise ratio of $5dB \sim 30dB$. The hybrid matrix estimation algorithm based on single source point detection and clustering in the literature is a commonly used algorithm to solve underdetermined blind source separation, and it is also the main method for frequency hopping network station sorting in underdetermined linear delay hybrid model. The authors introduce the Davis-Boulding cluster

evaluation criterion to address the known limitation of the K-means method on the number of clusters

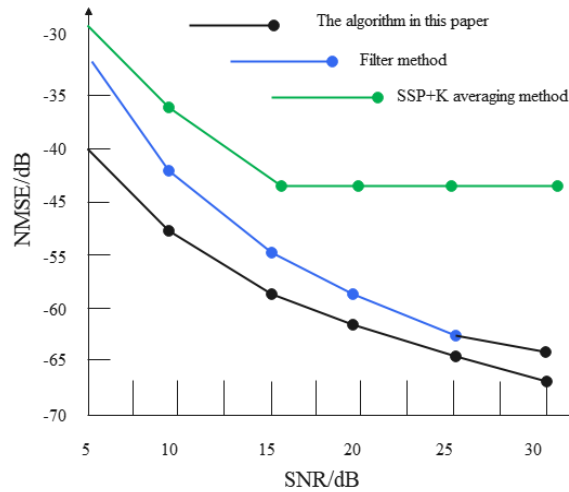


Figure 5: The curve diagram of the variation of NMSE with the signal-to-noise ratio in the mixed matrix estimation of the three algorithms.

From Figure 5, we can get that the hybrid matrix estimation algorithm based on single-source point detection and potential function clustering proposed in this paper has lower NMSE and higher estimation than the filtering method and the SSP+K-means algorithm precision. The K-means algorithm in the literature has poor robustness and low clustering accuracy, resulting in low overall performance of the algorithm.

2.4 Discussion on Hybrid Matrix Estimation in Synchronous Non-Orthogonal Networking

Different from synchronous orthogonal networking, synchronous non-orthogonal networking allows different frequency hopping network stations to use the same frequency at certain times. Since the feature information of high-density buildings in the source villages with the same frequency acts simultaneously at the time-frequency point $P(t_p, f_q)$, which does not satisfy the sparsity assumption, the above single-source point-based time-frequency analysis method cannot accurately estimate the mixing matrix.

We analyze this issue in two cases

- (1) There is a one-hop orthogonality of carrier frequencies for feature information of rural high-density building complexes

The mixture matrix is still estimated by the mixture matrix estimation algorithm in this paper. In an orthogonal one-hop, the value calculated by formula (28) can be used as DOA estimation, and the number is the same as the number of feature information of high-density buildings in the source village. In non-orthogonal hops, since the sparsity assumption is not satisfied, the θ value calculated from the feature information of the same-frequency rural high-density building group is the same, and it cannot be used as an estimate of DOA. Moreover, the number of θ is less than the number of feature information of high-density building groups in the source village.

According to the method in Section 1.2, the DoA of the feature information of each hop of rural high-density buildings is estimated. The number of DOA estimates of each hop data is compared, and the number of hops of data equal to the number of feature information of high-density buildings in the source village is selected. The mean value of the DOA corresponding to the same frequency f_n is used as the DOA estimate value of the feature information $s_n(t)$ of the high-density building group in the source village.

For the DOA values of non-orthogonal hops, we modify them according to the estimated DOA values within the quadrature hops. The specific methods are as follows:

If it is assumed that there are four source rural high-density building groups feature information $s_1(t), s_2(t), s_3(t), s_4(t)$, and $s_1(t)$ and $s_2(t)$ are in the same frequency, $\theta_1, \theta_2, \theta_3, \theta_4$ is the DOA estimated within the orthogonal hop, and $\theta_1', \theta_2', \theta_3'$ is the DOA estimated within the non-orthogonal hop. If there is $\theta_1' = \theta_1, \theta_2' = \theta_2$, θ_3' is a dummy value, which should be removed, and θ_3, θ_4 is added to the DOA estimate.

(2) The frequency of feature information of all high-density building groups in jumping villages is non-orthogonal

If the feature information frequencies of the n th and l th source rural high-density building groups within a hop are the same, a frequency collision will be formed. At the same time, the sum of the frequency collisions of the feature information of all the n and l th source rural high-density building

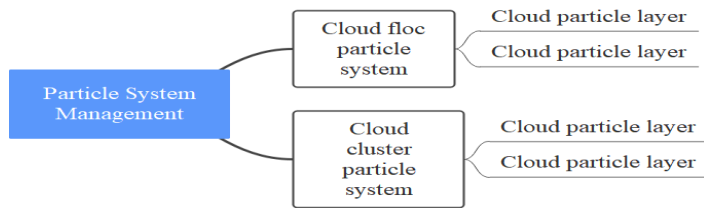
groups in a frequency hopping sequence period is defined as $H_{n,l}(l \neq n)$. Similarly, in a frequency hopping sequence period, the sum of the frequency collisions of the feature information of all hop n, l, \dots, p -th source rural high-density building groups is $H_{n,l,\dots,p}(n \neq l \neq \dots \neq p)$.

$$H < \frac{N}{2}$$

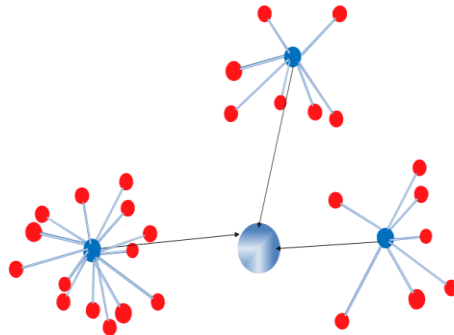
For any H , when $\frac{N}{2}$ is satisfied, the DOA of all hop data can be corrected. Among them, N is the number of feature information of high-density buildings in the source village.

3 RESEARCH ON PLANNING METHOD OF RURAL HIGH-DENSITY BUILDING GROUP BASED ON TREE STRUCTURE SIMULATION ALGORITHM

In the 3D cloud simulation system, the properties of particles mainly include their center position, radius, transparency and so on. A large number of particles are filled into the simulated three-dimensional volume space to obtain a simulated cloud. There are many types of clouds in the real world, cirrus, cumulus, stratus, etc. each have unique features. Therefore, the three-dimensional cloud simulation particle system in this paper must have a certain degree of flexibility and controllability, and users can simulate various types of clouds by only adjusting some parameters. In order to improve the simulation ability of particle system, in some special cases, it is generally considered to adopt multi-level particle system. Burg created the idea of advanced particle system and proposed a multi-level particle system. In this consideration, in order to better simulate the effect of cloud generation and drift, this paper decided to use a secondary particle system. The first-level cloud particle system (tree structure particle system) mainly simulates the basic structure and dynamic flow effect of clouds, and the second-level cloud floc particle system simulates the cloud generation and drifting effect. The schematic diagram of the particle system structure of the 3D cloud simulation is shown in Figure 6(a). The schematic diagram of the tree-structured particle system is shown in Figure 6(b).



(a) Schematic diagram of the particle system structure



(b) Schematic diagram of the tree-structured particle system

Figure 6: Tree structure simulation algorithm.

The ultimate goal of building group planning is to use the tree structure to evaluate the parameters of different dimensions of the differential image to determine the density function. The process includes the input of input variables, the selection of the optimal wide window, etc. The output value is the final function of density planning, which is the planning result. The overall process is shown in Figure 7.

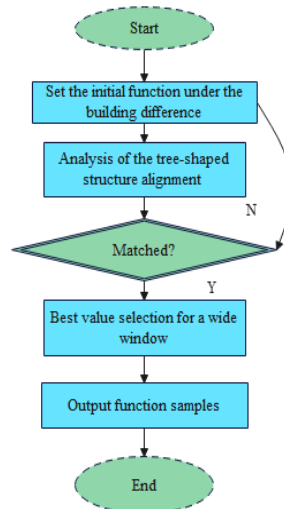


Figure 7: Flow chart of architectural planning.

This paper verifies the effect of the planning method for high-density rural buildings based on the tree structure simulation algorithm proposed in this paper. Moreover, this paper conducts multi-group simulations in combination with the planning requirements of building groups, counts the planning effect of high-density building groups in rural areas based on the tree structure simulation algorithm, and evaluates the effect, as shown in Table 1.

<i>NO.</i>	<i>Architectural Planning</i>	<i>NO.</i>	<i>Architectural Planning</i>
1	87.146	17	82.322
2	84.811	18	83.855
3	84.579	19	82.537
4	83.046	20	89.084
5	88.097	21	83.763
6	85.995	22	82.510
7	82.870	23	83.760
8	89.051	24	88.167
9	85.639	25	83.470
10	87.983	26	85.278
11	84.938	27	89.312
12	85.649	28	87.155
13	87.752	29	82.506
14	85.415	30	82.468
15	88.465	31	89.416
16	84.452	32	87.425

Table 1: Verification of the effect of planning method of rural high-density building groups based on tree structure simulation algorithm.

Through the simulation experiment research, it is verified that the planning method of rural high-density building groups based on the tree structure simulation algorithm can effectively improve the planning effect.

4 CONCLUSION

At present, the existing rural high-density building planning methods can generally be divided into frame difference method, background subtraction method and optical flow method according to image division. The above methods realize the planning of rural building groups through the evaluation function with the support of the background image. However, due to the difference in the accuracy of the planning functions, the final planning effect is not ideal. Therefore, this paper designs and adopts a building group planning strategy based on tree structure simulation. It relies on the difference image and tree structure simulation compatibility results to output the evaluation function to realize the building planning of the rural high density function. This paper combines the tree structure simulation algorithm to analyze the planning and analysis of rural high-density building groups, and improves the planning effect of rural high-density building groups through intelligent methods. Through the simulation experiment research, it is verified that the planning method of rural high-density building groups based on the tree structure simulation algorithm can effectively improve the planning effect.

Jingwen Wang, <https://orcid.org/0009-0001-3591-1619>
 Zhaozhao Huang, <https://orcid.org/0009-0006-8911-6019>

REFERENCES

- [1] Abed, H. R.; Hatem, W. A.; Jasim, N. A.: Adopting BIM technology in fall prevention plans, *Civil Engineering Journal*, 5(10), 2019, 2270-2281. <https://doi.org/10.28991/cej-2019-03091410>
- [2] Al-Ashmori, Y. Y.; Othman, I.; Rahmawati, Y.; Amran, Y. M.; Sabah, S. A.; Rafindadi, A. D. U.; Mikić, M.: BIM benefits and its influence on the BIM implementation in Malaysia, *Ain Shams Engineering Journal*, 11(4), 2020, 1013-1019. <https://doi.org/10.1016/j.asej.2020.02.002>
- [3] Chen, C. J.; Chen, S. Y.; Li, S. H.; Chiu, H. T.: Green BIM-based building energy performance analysis, *Computer-Aided Design and Applications*, 14(5), 2017, 650-660. <https://doi.org/10.1080/16864360.2016.1273582>
- [4] Fadeyi, M. O.: The role of building information modeling (BIM) in delivering the sustainable building value, *International Journal of Sustainable Built Environment*, 6(2), 2017, 711-722. <https://doi.org/10.1016/j.ijse.2017.08.003>
- [5] Joblot, L.; Paviot, T.; Deneux, D.; Lamouri, S.: Literature review of Building Information Modeling (BIM) intended for the purpose of renovation projects, *IFAC-Papers OnLine*, 50(1), 2017, 10518-10525. <https://doi.org/10.1016/j.ifacol.2017.08.1298>
- [6] Kim, I.; Choi, J.; Teo, E. A. L.; Sun, H.: Development of K-BIM e-Submission prototypical system for the openBIM-based building permit framework, *Journal of Civil Engineering and Management*, 26(8), 2020, 744-756. <https://doi.org/10.3846/jcem.2020.13756>
- [7] Kim, Y. C.; Hong, W. H.; Park, J. W.; Cha, G. W.: An estimation framework for building information modeling (BIM)-based demolition waste by type, *Waste Management & Research*, 35(12), 2017, 1285-1295. <https://doi.org/10.1177/0734242X17736381>
- [8] Kocakaya, M. N.: Building information management (BIM), a new approach to project management, *Journal of sustainable construction materials and technologies*, 4(1), 2019, 323-332. <https://doi.org/10.29187/jscmt.2019.36>
- [9] Koutamanis, A.; Heuer, J.; Könings, K. D.: A visual information tool for user participation during the lifecycle of school building design: BIM, *European Journal of Education*, 52(3), 2017, 295-305. <https://doi.org/10.1111/ejed.12226>
- [10] Mandičák, T.; Mesároš, P.; Tkáč, M.: Impact of management decisions based on managerial competencies and skills developed through BIM technology on performance of construction enterprises, *Pollack Periodica*, 13(3), 2018, 131-140. <https://doi.org/10.1556/606.2018.13.3.13>
- [11] Noor, S. M.; Junaidi, S. R.; Ramly, M. K. A.: Adoption of building information modelling (bim): factors contribution and benefits, *Journal of Information System and Technology Management*, 3(10), 2018, 47-63.
- [12] Okakpu, A.; GhaffarianHoseini, A.; Tookey, J.; Haar, J.; Ghaffarianhoseini, A.; Rehman, A.: A proposed framework to investigate effective BIM adoption for refurbishment of building projects, *Architectural Science Review*, 61(6), 2018, 467-479. <https://doi.org/10.1080/00038628.2018.1522585>
- [13] Papadonikolaki, E.; van Oel, C.; Kagioglou, M.: Organising and Managing boundaries: A structural view of collaboration with Building Information Modelling (BIM), *International journal of project management*, 37(3), 2019, 378-394. <https://doi.org/10.1016/j.ijproman.2019.01.010>
- [14] Ustinovichius, L.; Popov, V.; Cepurnaite, J.; Vilutienė, T.; Samofalov, M.; Miedziński, C.: BIM-based process management model for building design and refurbishment, *Archives of Civil and Mechanical Engineering*, 18(4), 2018, 1136-1149. <https://doi.org/10.1016/j.acme.2018.02.004>

- [15] Ustinovičius, L.; Puzinas, A.; Starynina, J.; Vaišnoras, M.; Černiavskaja, O.; Kontrimovičius, R.: Challenges of BIM technology application in project planning, *Engineering Management in Production and Services*, 10(2), 2018, 15-28. <https://doi.org/10.2478/emj-2018-0008>
- [16] Wei, T.; Chen, Y.: Green building design based on BIM and value engineering, *Journal of Ambient Intelligence and Humanized Computing*, 11(9), 2020, 3699-3706. <https://doi.org/10.1007/s12652-019-01556-z>
- [17] Wu, P., Jin, R., Xu, Y., Lin, F., Dong, Y., & Pan, Z. (2021). The analysis of barriers to bim implementation for industrialized building construction: a China study, *Journal of Civil Engineering and Management*, 27(1), 1-13. <https://doi.org/10.3846/jcem.2021.14105>
- [18] Xu, J.; Li, B. K.; Luo, S. M.: Practice and exploration on teaching reform of engineering project management course in universities based on BIM simulation technology, *EURASIA Journal of Mathematics, Science and Technology Education*, 14(5), 2018, 1827-1835. <https://doi.org/10.29333/ejmste/85417>